Cell. Mol. Life Sci. (2011) 68:1799–1813
DOI 10.1007/s00018-010-0539-8

Cellular and Molecular Life Sciences

RESEARCH ARTICLE

Cooperative interactions between odorant-binding proteins of *Anopheles gambiae*

Huili Qiao · Xiaoli He · Danuta Schymura · Liping Ban · Linda Field · Francesca Romana Dani · Elena Michelucci · Beniamino Caputo · Alessandra della Torre · Kostas Iatrou · Jing-Jiang Zhou · Jürgen Krieger · Paolo Pelosi

Received: 9 July 2010 / Revised: 23 August 2010 / Accepted: 23 September 2010 / Published online: 19 October 2010

Abstract To understand olfactory discrimination in *Anopheles gambiae*, we made six purified recombinant OBPs and investigated their ligand-binding properties. All OBPs were expressed in bacteria with additional production of OBP47 in the yeast *Kluveromyces lactis*. Ligand-binding experiments, performed with a diverse set of organic compounds, revealed marked differences between the OBPs. Using the fluorescent probe *N*-phenyl-1-naphthylamine, we also measured the binding curves for binary mixtures of OBPs and obtained, in some cases, unexpected behaviour, which could only be explained by the OBPs forming heterodimers with binding characteristics different from those of the component proteins. This shows that OBPs in mosquitoes can form complexes with novel ligand specificities, thus amplifying the repertoire of OBPs and the number of semiochemicals that can be discriminated. Confirmation of the likely role of heterodimers was demonstrated by in situ hybridisation, suggesting that OBP1 and OBP4 are co-expressed in some antennal sensilla of *A. gambiae*.

Keywords Odorant-binding protein · *Anopheles gambiae* · Protein expression · Fluorescent binding assay · Protein association · Semiochemicals · In situ hybridisation

Abbreviations

OBP	Odorant-binding protein
MALDI-TOF	Matrix-assisted laser desorption ionisation-time of flight
ESI-MS	Electrospray ionisation mass spectrometry
FITC	Phenyl-isothiocyanate
1-NPN	*N*-phenyl-1-naphthylamine

Dedicated to the memory of the late Harald Biessmann, our colleague and dear friend, who completed the cloning and initial characterization of the majority of *Anopheles gambiae* odorant-binding proteins.

H. Qiao and X. He contributed equally to the work.

Electronic supplementary material The online version of this article (doi:10.1007/s00018-010-0539-8) contains supplementary material, which is available to authorized users.

H. Qiao · P. Pelosi (✉)
Department of Biology and Agricultural Plants, University of Pisa, Via S. Michele, 4, 56124 Pisa, Italy
e-mail: ppelosi@agr.unipi.it

X. He · L. Ban · L. Field · J.-J. Zhou (✉)
Department of Biological Chemistry, Rothamsted Research, Harpenden, UK
e-mail: jing-jiang.zhou@bbsrc.ac.uk

D. Schymura · J. Krieger
Institute of Physiology, University of Hohenheim, Stuttgart, Germany

F. R. Dani · E. Michelucci
Centro Interdipartimentale di Spettrometria di Massa, University of Firenze, Florence, Italy

B. Caputo · A. d. Torre
Dipartimento di Scienze di Sanità Pubblica, Istituto Pasteur-Fondazione Cenci-Bolognetti, Sezione di Parassitologia, University 'Sapienza', Rome, Italy

K. Iatrou
Insect Molecular Genetics and Biotechnology Group, Institute of Biology, National Centre for Scientific Research 'Demokritos', Athens, Greece

Introduction

Mosquitoes are vectors of many diseases, such as malaria, dengue and yellow fever, thus posing a major threat to human health worldwide, particularly in developing countries. At present, vector control is dependent on treatment with insecticides either on bed nets or as indoor residual sprays, although alternative approaches, based on the use of semiochemicals, are being investigated [1]. As for all other insects, mosquito host location uses olfactory cues, particularly carbon dioxide, a major attractant, together with lactic acid and other volatiles produced by the host that can potentiate their behaviour. Interestingly, human sweat contains chemicals that have been reported to act as repellents of mosquitoes [2, 3].

Synthetic mosquito repellents are widely used, but their mode of action remains unclear. DEET and Icaridin are the most commonly used in commercial products, which contain high levels (10–20%) of the active ingredient. Recently, it has been proposed that they also have insecticidal action, as acetylcholine esterase inhibitors [4]. This raises some concern as to the safety of these products for humans and other animals.

A number of other volatile compounds have been reported as mosquito repellents, such as nepetalactone, cinnanic aldehyde, citronellal and isolongifolenone [5–8], but all of these are effective only at very high concentrations. The structural diversity of the compounds and the lack of data on their mode of action mean that there is no rationale to allow the design of chemicals with improved repellency effect. Thus, the focus of this research, to devise alternative strategies for mosquito control, is on the biochemistry of olfaction. In particular, the proteins responsible for detecting and recognising host odours and pheromones are being investigated in order to elucidate the olfactory code of these insects. The genome of the main malaria vector *Anopheles gambiae* has 79 and 76 genes encoding putative olfactory receptors and gustatory receptors, respectively, as well as 60 genes for putative odorant-binding proteins (OBPs) [9]. Very recently, the screening of ligand specificity for 50 olfactory receptors has been published, a major work, representing a solid and important basis of information for future research [10, 11].

We have focused our attention on the other protein partners involved in odour recognition, i.e., the OBPs [12–14]. In the last few years the proposed role of OBPs has been raised from that of simple odorant carriers to that of being responsible, together with the membrane-bound olfactory receptors, for recognition and discrimination of odorant stimuli. In the silkmoth *Bombyx mori*, the activation of the pheromone receptor requires the presence of the corresponding pheromone-binding proteins [15]. Silencing of the gene encoding LUSH, one of the OBPs of *Drosophila melanogaster*, suppresses both electrophysiological and behavioural responses to vaccenyl acetate, the male pheromone for this species [16]. Moreover, it has been demonstrated that vaccenyl acetate, upon binding to LUSH, induces a conformational change in the structure of this protein, which allows stimulation of the corresponding olfactory receptor. This was elegantly demonstrated by a modified LUSH protein that mimics the structure of the LUSH/vaccenyl acetate complex and is able to activate the olfactory receptor even in the absence of the pheromone [17].

Another elegant study has demonstrated the role of two OBPs (OBP57d and OBP57e) in the detection of two fatty acids that act as oviposition attractants in *Drosophila sechellia*. The same fatty acids act as repellents for *D. melanogaster* (and other *Drosophila* species), and experiments where the two genes encoding the OBPs were exchanged between two species of *Drosophila* produced, to some extent, a switch in behaviour, making the two fatty acids repellents of *D. sechellia* and attractants for *D. simulans* [18].

More recently and specifically in mosquitoes, it has been shown that silencing of the gene encoding OBP1 in *A. gambiae* [19] and in *Culex quinquefasciatus* [20] suppresses electrophysiological responses to indole, showing that in both species OBP1 is essential for the perception of indole.

Overall, results to date confirm the important role of OBPs in odour perception and discrimination, and this, together with the great impact of disease vectors on human health, prompted us to study the specificity of binding between OBPs and olfactory ligands in *A. gambiae*. Given the enormous amount of work that would be involved in analysing all 60 putative OBPs, we selected for study those that have been found to be the most abundantly expressed in olfactory organs [1, 9, 21–24]. Molecular biology techniques have shown that only a small set of OBP-encoding genes are expressed in sensory organs at relatively high levels. In particular, those most abundantly expressed in female antennae are the classic OBPs 1, 3, 4, 5, 7, 9 and 17 and two of the C-plus OBPs, 47 and 48. In some cases the expression of the OBP genes is upregulated or downregulated after a blood meal, indicating that the corresponding proteins might be involved in host recognition [23]. The same authors have reported that each OBP is differentially expressed according to tissue and sex, while a substantial number of them (mainly belonging to the so-called "atypical OBPs") are not expressed in any part of the body of either sex [9].

Another important aspect of studying the contribution of OBPs in odour perception is the possibility that different OBPs might form heterodimers. Indeed, interactions between OBP48 and some classic OBPs, as well as between OBP1 and OBP4, have been reported using co-immunoprecipitation methods and cross-linking studies [22].

In the current study we have investigated the binding properties of selected OBPs of *A. gambiae*, expressed in heterologous systems, towards a number of potential semiochemicals using ligand-binding assays. We also provide data suggesting that OBP4 interacts with OBP1 and with OBP3, generating heterodimers with novel characteristics. Finally, our in situ hybridisation experiments indicate that OBP1 and OBP4 are co-expressed in some antennal sensilla of *A. gambiae*.

Materials and methods

Insects

The *A. gambiae* used for most assays belonged to the GACAM-ST colony maintained in the Department of Public Health Sciences at the University of Rome, Sapienza (Italy). This colony originated from *A. gambiae* M-molecular form [sensu della Torre [25] females collected in Cameroon in 2004 and selected for a standard polytene complement (Xag, 2R+, 2L+, 3R+, 3L+)] [26]. All insects analysed were 2–4 days old. Specimens were killed by freezing at −20°C and kept at this temperature prior to analyses. Whole-mount in situ hybridisation experiments were carried out on *A. gambiae* molecular form S (strain Kisumu) kindly provided by Bayer CropScience (Monheim, Germany). Larvae were reared at 28 ± 1°C and 80 ± 10 RH and fed with cat pellets, and adults were maintained at 26 ± 1°C and 70 ± 10 RH and fed on 10% sucrose; both were kept in a day:night cycle of 12:12 h.

Reagents

All enzymes were from New England Biolabs. Oligonucleotides were custom synthesised at Eurofins MWG GmbH, Ebersberg, Germany. All other chemicals were either purchased from Sigma-Aldrich and were of reagent grade, or were synthesised in house using conventional synthesis routes.

Cloning and sequencing

Plasmids containing the appropriate OBP cDNAs were subjected to PCR, using primers encoding the first and the last six amino acids of each sequence, flanked by *Nde*I and *Eco*RI restriction sites in the forward and reverse primer, respectively. The crude PCR products were ligated into a pGEM (Promega) vector, using a 1:5 (plasmid:insert) molar ratio and incubating the mixture overnight at room temperature. After transformation of *E. coli* XL-1 Blue competent cells with the ligation products, positive colonies were selected by PCR using the plasmid's primers SP6 and T7 and grown in LB/ampicillin medium. DNA was extracted using the GFX Micro Plasmid Prep (GE-Healthcare) kit and custom sequenced at Eurofins MWG (Martinsried, Germany).

Cloning in expression vectors

pGEM plasmids containing the appropriate sequences were digested with *Nde*I and *Eco*RI restriction enzymes for 2 h at 37°C, and the digestion products were separated on agarose gels. The fragments were purified from the gel and ligated into the expression vector pET5b (Novagen, Darmstadt, Germany), previously linearized with the same enzymes. The inserts in the resulting plasmids were sequenced to confirm that they encoded the correct mature proteins.

Bacterial expression of the proteins

For expression of recombinant proteins, each pET-5b vector containing the appropriate OBP sequence was used to transform *E. coli* BL21(DE3)pLysS cells. Protein expression was induced by addition of IPTG to a final concentration of 0.4 mM when the culture had reached a value of $O.D_{600} = 0.8$. Cells were grown for a further 2 h at 37°C, then harvested by centrifugation and sonicated. After further centrifugation, OBPs, present in the pellets (from 1 of culture) as inclusion bodies were solubilised by dissolving the pellet in 10 ml of 8 M urea, 1 mM DTT in 50 mM Tris buffer, pH 7.4, then diluting to 100 ml with Tris buffer and dialysing three times against Tris buffer. The OBPs were then purified using combinations of chromatographic steps anion-exchange resins, such as DE-52 (Whatman), QFF or Mono-Q (GE Healthcare), followed by gel filtration on Sephacryl-100 or Superose-12 (GE Healthcare) along with standard protocols previously adopted for other OBPs [27, 28].

Cloning and expression in *K. lactis*

Introduction of the linearized OBP47 expression cassette into *K. lactis* cells was achieved by chemical transformation using the *K. lactis* GG799 competent cells and NEB yeast transformation reagent. Transformants were selected by growth on YCB agar medium containing acetamide and the colonies analysed by PCR. Positive colonies were resuspended in 2 ml YPGal medium and shaken at 200–250 rpm and 30°C. Analysis of culture supernatant was performed after 2, 3 and 4 days of incubation to determine the best time to optimise protein yield.

Digestion with PNGase

Samples of OBP47 expressed in yeast (10 µg) in 100 µl 50 mM Tris-Cl pH 7.4 buffer were treated with 2 µl

(10 units) of PNGaseF at 37°C for 2 h. The digestion product was analysed by SDS-PAGE followed by Western blot analysis and MALDI mass spectrometry.

Preparation of antisera

Antisera were obtained in adult rabbits after repeated injections of the recombinant proteins emulsified in Freund's adjuvant and used without further purification. The immunisations were performed according to the protocol approved by the University of Pisa ethics committee.

Western blot analysis

After electrophoretic separation of proteins under denaturing conditions (14% SDS-PAGE), duplicate gels were stained with 0.1% Coomassie blue G250 in 10% acetic acid, 25% ethanol or electroblotted onto Trans-Blot nitrocellulose membrane (Bio-Rad Lab) by the procedure of [29]. After treatment with 2% powdered skimmed milk/0.05% Tween 20 in PBS overnight, the membrane was incubated with the crude antiserum against the relevant OBP at a dilution of 1:500 (2 h) and then with goat anti-(rabbit IgG) horseradish peroxidase conjugate (dilution 1:1,000; 1 h). Immunoreacting bands were detected by treatment with 4-chloro-1-naphthol and hydrogen peroxide.

MALDI mass spectrometry

Protein samples were analysed on a MALDI-TOF/TOF mass spectrometer Ultraflex III (Bruker Daltonics, Bremen, Germany) using Flex Control^{TM} 3.0 as the data acquisition software. A 1 µl volume of the sample was mixed with 1 µl of the matrix (sinapinic acid 10 mg/ml in CH_3CN:H_2O, 0.1% TFA, 70:30) on the target and allowed to dry. Spectra were acquired in linear mode over the *m/z* range 5,000–20,000. The instrument parameters were chosen by setting ion source 1 at 25 kV, ion source 2 at 23.45 kV, lens at 6.0 kV and pulsed ion extraction at 80 ns. The instrument was externally calibrated prior to analysis using the Bruker Protein I calibrant standard kit (5,000–17,000 Da) [30].

High resolution mass spectrometric analysis

A 5 μM solution of OBP47 expressed in *E.coli* was prepared after a 20-fold dilution with HCOOH 0.1%. ESI-MS spectra were recorded by direct introduction at 5 µl/min flow rate in an LTQ-Orbitrap high-resolution mass spectrometer (Thermo, San Jose, CA), equipped with a conventional ESI source. The spray voltage was 3.1 kV, the capillary voltage was 45 V, the capillary temperature was kept at 220°C, and the tube lens voltage was 230 V. The sheath and the auxiliary gases were set, respectively, at 17 (arbitrary units) and 1 (arbitrary units). For data acquisition, Xcalibur 2.0. software (Thermo) was used, and monoisotopic and average deconvoluted masses were obtained using the integrated Xtract tool. For spectra acquisition a nominal resolution (at *m/z* 400) of 100,000 was used.

The experimental isotope patterns in charge state 12^+ were compared with the theoretical patterns of the protein molecular formula as predicted with 6 or 5 disulfide bridges.

Fluorescence measurements

Emission fluorescence spectra were recorded on a Jasco FP-750 instrument at 25°C in a right angle configuration, with a 1-cm light path quartz cuvette and 5-nm slits for both excitation and emission. The protein was dissolved in 50 mM Tris-HCl buffer, pH 7.4, and ligands were added as 1 mM methanol solutions.

Fluorescence binding assays

To measure the affinity of the fluorescent ligand 1-NPN to each OBP, a 2 µM solution of the protein in 50 mM Tris-HCl, pH 7.4, was titrated with aliquots of 1 mM ligand in methanol to final concentrations of 2–16 µM. The probe was excited at 337 nm, and emission spectra were recorded between 380 and 450 nm. The affinity of other ligands was measured in competitive binding assays, using 1-NPN as the fluorescent reporter at 2 µM concentration and 2–16 µM concentrations for each competitor.

For determining binding constants, the intensity values, corresponding to the maximum of fluorescence emission were plotted against free ligand concentrations. Bound ligand was evaluated from the values of fluorescence intensity assuming that the protein was 100% active, with a stoichiometry of 1:1 protein:ligand at saturation. The curves were linearised using Scatchard plots. Dissociation constants of the competitors were calculated from the corresponding IC_{50} values, using the equation: $K_D = [IC_{50}]/1 + [1\text{-NPN}]/K_{1\text{-NPN}}$, where [1-NPN] is the free concentration of 1-NPN and $K_{1\text{-NPN}}$ is the dissociation constant of the complex protein/1-NPN.

Double whole-mount in situ hybridisation (double WM-FISH)

Antennae were dissected from 1- to 3-day old cold anaesthetised mosquitoes and fixed for 20–24 h at 6°C in 4% paraformaldehyde in 0.1 M Na_2CO_3, pH 9.5, 0.03% Triton X-100. After a wash at room temperature for 1 min in PBS (phosphate-buffered saline = 0.85% NaCl,

1.4 mM KH_2PO_4, 8 mM Na_2HPO_4, pH 7.1) with 0.03% Triton X-100, the antennae were incubated for 10 min in 0.2 M HCl, 0.03% Triton X-100. Subsequently, antennae were washed for 2 min in PBS with 1% Triton X-100 and transferred to whole mount in situ hybridisation solution (50% formamide, 5× SSC, 1× Denhardts reagent, 50 µg/ml yeast RNA, 1% Tween 20, 0.1% Chaps, 5 mM EDTA pH 8.0). If not prehybridised directly, antennae were stored at 6°C in the solution. Prehybridisation was performed at 55°C for 6 h, followed by incubation for at least 48 h at the same temperature in hybridisation solution containing the labelled OBP antisense RNA probes. Labelled riboprobes of OBP1 [digoxigenin (DIG)-labelled] and OBP4 (biotin-labelled) were transcribed from linearised plasmids containing the coding regions of the OBPs using a T3/T7 RNA transcription system (Roche) and recommended protocols. Posthybridisation, antenna were washed four times for 15 min each in 0.1× SSC, 0.03% Triton X-100 at 60°C and then treated with 1% blocking reagent (Roche) in TBS (100 mM Tris, pH 7.5, 150 mM NaCl), 0.03% Triton X-100 for 5 h at 6°C. The DIG-labelled probe was detected by incubation for at least 48 h with an anti-DIG alkaline phospatase-conjugated antibody (Roche) diluted 1:500 in TBS, 0.03% Triton X-100 with 1% blocking reagent; for detection of the biotin-labelled probe a strepavidin horseradish peroxidase-conjugate (1:100, TSA kit, Perkin Elmer) was included in the same solution. After washing five times for 10 min each in TBS with 0.05% Tween at room temperature, the DIG-labelled probe was visualised by incubation with HNPP [Roche; 1:100 in DAP-buffer (100 mM Tris, pH 8.0, 100 mM NaCl, 50 mM $MgCl_2$] for 5 h in the dark at 6°C. After three 5-min washes in TBS with 0.05% Tween, the TSA kit/FITC development was conducted for 17–18 h at 6°C in the dark to visualise the biotin-labelled probe. Following a short wash in PBS the antennae were mounted in moviol (10% polyvinylalcohol 4-88, 20 glycerol in PBS). All incubations and washes were made in a volume of 0.25 ml (in Quali-PCR tubes, Kisker, Germany) with slow rotation or moderate shaking. The binding of the probes was analysed for epifluorescence using a Zeiss LSM510 Meta laser scanning microscope (Zeiss, Oberkochen, Germany).

Molecular modelling

Three-dimensional models of *A. gambiae* OBP3 and OBP4 were generated using the on-line programme SWISS MODEL [31–33]. Models were displayed using the SwissPdb Viewer programme "Deep-View" [32] (http://www.expasy.org/spdbv/).

Results and discussion

Choice of the proteins

We selected six *A. gambiae* OBPs for our study, numbered in the Swiss-Prot data base as 1, 3, 4, 12, 19 and 47. They are all classic OBPs (with the conserved pattern of six cysteines), except for OBP47, which is much longer (173 amino acids instead of 119–132 for the others) and contains 13 cysteines. The genes encoding these OBPs have all been shown to be expressed at relatively high levels by Northern blot and microarray experiments [1, 9, 21] with all, except for OBP12 and OBP19, being in the top 10 OBPs most expressed in female antennae. OBP12 was included because its expression is almost three times higher in female antennae than in males, and OBP19, together with OBP47, is one of the few OBPs selectively expressed in the head.

Some of the OBPs chosen have interesting structural relationships with their counterparts in other mosquito species and in *Drosophila*. In particular, OBP1 and OBP3 are the orthologues of *D. melanogaster* OS-E and OS-F, respectively, and OBP4 is structurally similar to *Drosophila* LUSH. It is particularly interesting that these three proteins of *Drosophila* have been observed to be expressed in the same chemosensilla [34, 35].

Expression, purification and partial structural characterisation

All six *A. gambiae* OBPs were expressed in *E. coli* and gave good yields of the recombinant proteins (20 mg/l). To minimise the effect of His-tags (or other sequences to allow affinity purification) on ligand-binding assays, we made constructs coding only for a starting methionine in addition to the mature protein sequence. As observed with most insect OBPs, our recombinant proteins were present in the bacterial cells as insoluble inclusion bodies and had to be solubilised by denaturation and reduction. Although the conditions used in this process are particularly harsh, the unfolded OBPs can be renatured correctly as demonstrated in several cases by binding experiments, pairing of disulphide bridges and crystal structure [27, 36, 37]. OBP47, despite its length and the presence of 13 cysteine residues, was refolded into its active conformation as judged from its binding properties toward several ligands similar to those of other insect OBPs.

Purification of each OBP was accomplished using conventional techniques, combining anion-exchange chromatography with gel filtration. Figure 1 shows the electrophoretic analysis of both the crude expression products and samples of purified proteins for each of the

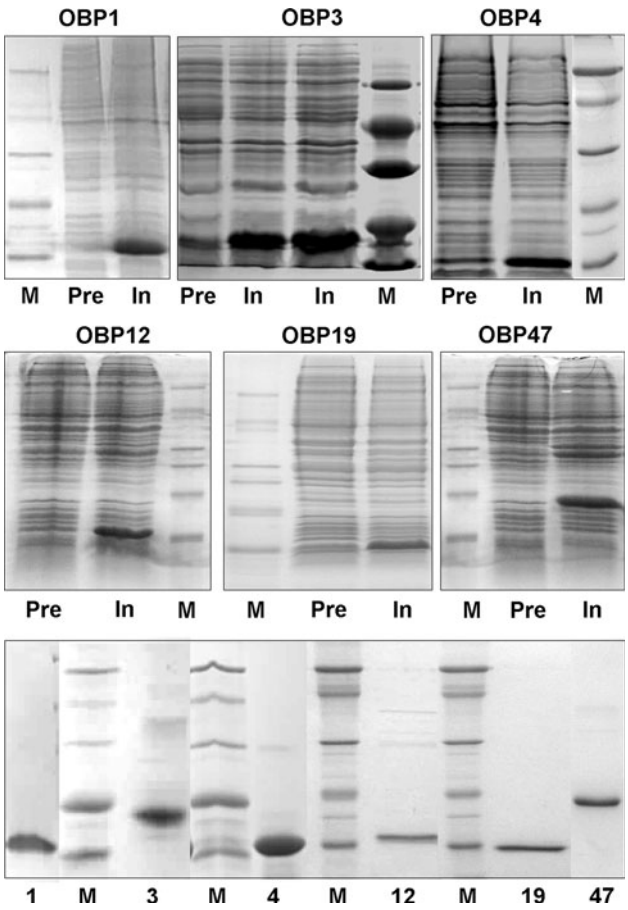

Fig. 1 Expression and purification of six OBPs of *Anopheles gambiae*. Upper two panels: electrophoretic analysis (SDS-PAGE) of crude bacterial pellets, each expressing one of the OBPs, before (*Pre*) and after (*In*) induction of the bacterial culture with IPTG. Lower panel: samples of purified OBPs. *M*: molecular weight markers of 66, 45, 29, 20 and 14 kDa

six OBPs. The correct folding of OBP1, OBP3 and OBP4 was also supported by the observation that these proteins, after denaturation and renaturation, migrate as single bands on a native PAGE (Figure S1).

We also expressed OBP47 in the yeast *K. lactis*, obtaining yields of around 20 mg of protein per litre. In this case, the protein was secreted in the medium in its soluble form and could be purified easily, representing by far the major protein component of the culture medium. The OBP47 prepared in yeast migrated with a higher molecular weight on SDS-PAGE than did the protein expressed in the bacterial system, suggesting that glycosylation could have been introduced. To verify this, a sample of the yeast-produced protein was digested with PNGase and the product analysed by SDS-PAGE followed by Western blot (Fig. 2), as well as by MALDI mass spectrometry (Fig. 3). The Western blot analysis, using a crude polyclonal antiserum against the bacterially expressed OBP47, showed the presence of a band in the digested sample, migrating with the

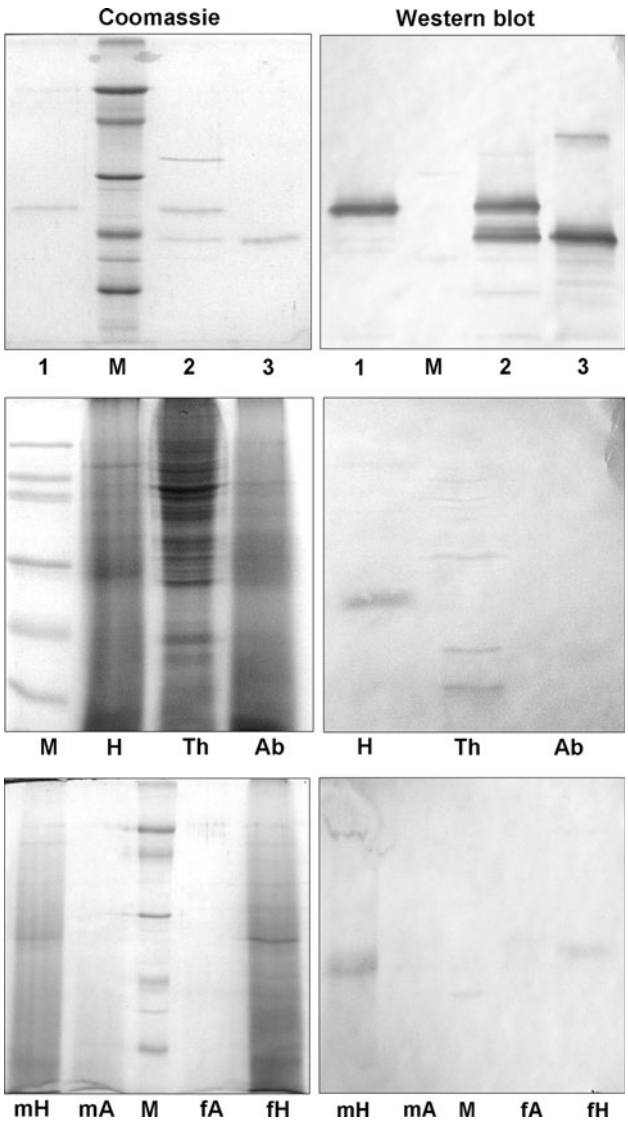

Fig. 2 Analysis and tissue expression of OBP47. *Upper panel*: OBP47 produced in the yeast *K. lactis* (*1*) migrating with an apparent molecular weight of about 22 kDa, whilst bacterial-expressed OBP47 (*3*) shows a mass of about 19 kDa, in agreement with the calculated value of 18,918 Da. Treatment of the yeast-expressed OBP47 with PNGase F (*2*) generates a band migrating with an apparent mass identical with that of the bacterial sample. *Middle panel*: Expression of OBP47 in head (*H*), thorax (*Th*) and abdomen (*Ab*) of *An. gambiae* (mixed sexes). Western blot analysis reveals the exclusive presence of OBP47 in the head. *Lower panel*: OBP47 is mostly expressed in heads without antennae of male (*mH*) and female (*fH*) mosquitoes, and is only barely detectable in the antennae of both sexes (*mA* and *fA*). *M*: molecular weight markers of 66, 45, 29, 20 and 14 kDa

same apparent mass as the bacterial OBP47 and indicating that the protein produced in yeast is glycosylated (Fig. 2). Likewise, the MALDI spectrum showed a main broad peak around mass 21,517.6, indicating a heterogeneous population of glycosylated OBP47 and a minor peak at mass 18,922.5, in agreement with the calculated molecular weight of the de-glycosylated protein, assuming the

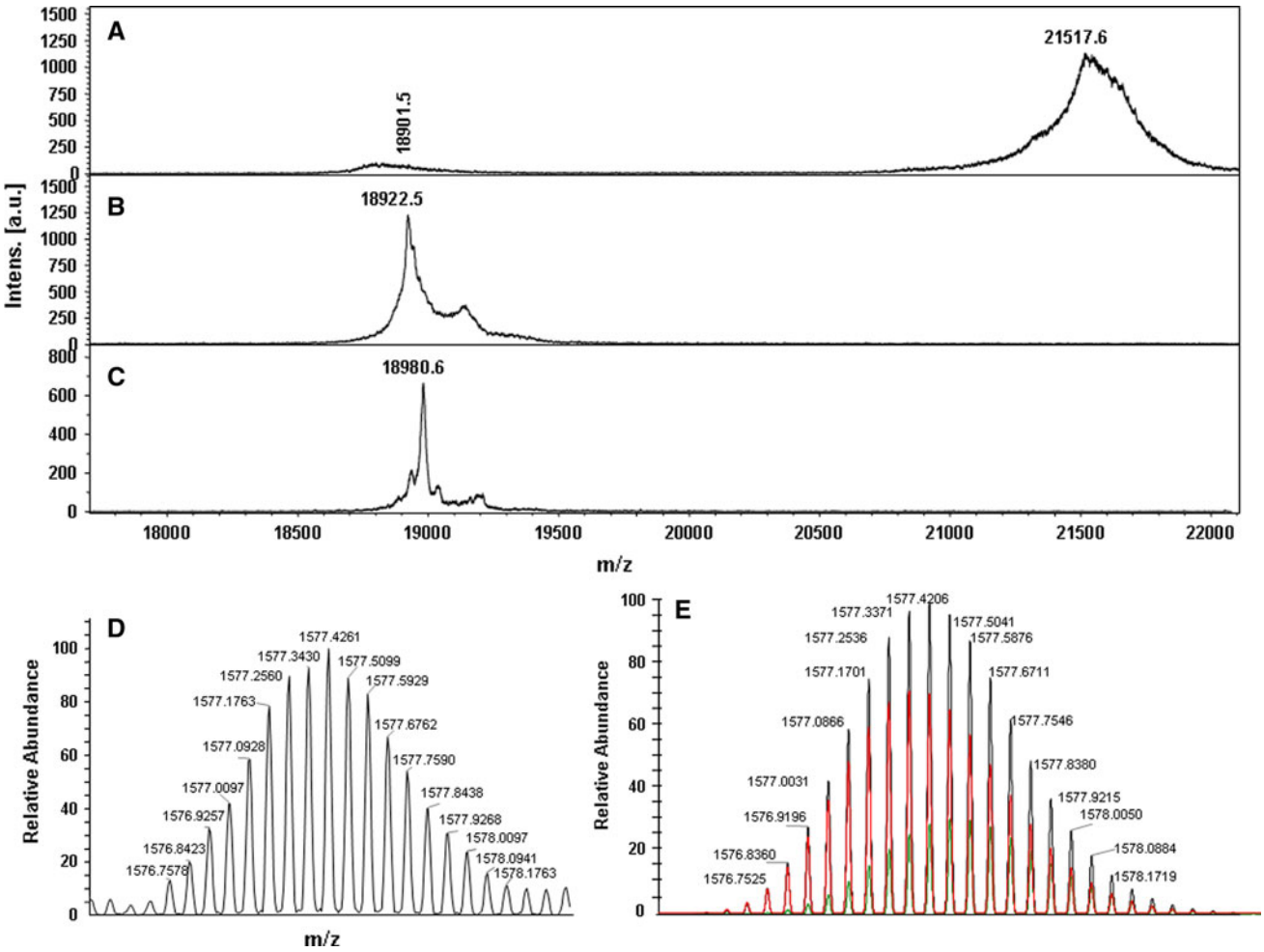

Fig. 3 **a** MALDI spectrum of OBP47 expressed in *K. lactis* and deglycosylated with PNGase; both the glycosylated and the deglycosylated forms are present, the glycosylated being predominant. **b** MALDI spectrum of OBP47 expressed in *E. coli*. **c** MALDI spectrum of OBP47 expressed in *E. coli* after cysteine carboamidomethylation. The mass difference corresponds to a single carboamidomethyl group introduced in the derivatised sample. Calculated masses for OBP47 expressed in *E. coli* (assuming the presence of six disulfide bridges) before and after carboamidomethylation are 18, 918 and 18,975, respectively. **d, e** Comparison of **d** the experimental spectrum of the 12^+ charge state of OBP47 expressed in *E. coli* and **e** the theoretical 12^+ charge state spectrum obtained by considering the protein to have six (in *red*) or 5 (in *green*) disulfide bridges in a ratio 7:3 (sum of the two spectra in *black*). Data were recorded on LTQ Orbitrap high resolution mass spectrometer

presence of six disulphide bridges (18,918). The same antiserum was also used to probe the expression of OBP47 in different parts of the adult mosquito, and the results clearly indicate that expression is restricted to the head of both sexes (Fig. 2). We can also observe that the OBP is present in mosquitoes in its glycosylated form, migrating with an apparent molecular weight of about 22 kDa. A second experiment showed that the expression of OBP47 is only a barely detectable in the antennae, with most of the reactivity being associated with heads without antennae (Fig. 2). This finding might suggest that OBP47 could be most abundantly present in mouth structures, such as palpi and proboscis, with a putative function in taste.

As a first contribution to a structural characterisation of OBP47, we investigated the number of free cysteines in the refolded protein. Derivatization of the bacteria-produced OBP with iodoacetamide gave a single molecular species with the MALDI mass spectrum giving a mass of 18,980.6 units (Fig. 3). The difference with respect to the non-derivitized protein (measured mass 18,922.5) is 58 units, accounting for a single cysteine residue being derivatised and indicating that only 1 of the 13 cysteines present in OBP47 is in its reduced form. To confirm this, and rule out the possibility of additional free cysteines buried in the core of the protein and hence not affected by the reagent, we also performed an exact measurement of the mass of the protein. In Fig. 3 the portion of the electrospray mass spectrum relative to the 12 charge ion is compared with the theoretical spectra calculated for the formulae $C_{825}H_{1309}N_{215}O_{249}S_{22}$ and $C_{825}H_{1311}N_{215}O_{249}S_{22}$

relative to the protein with, respectively, one and three free cysteines in a ratio of 7:3. This indicates that the most probable configuration of OBP47 is the one with a single free cysteine, as also suggested by the experiments performed with the derivatized protein.

Ligand-binding experiments

The six recombinant OBPs were then tested for their ligand-binding characteristics, using a number of small organic compounds in fluorescent displacement assays. First, affinity constants were measured for each protein to the fluorescent probe 1-NPN (*N*-phenyl-1-naphthylamine). All of the OBPs tested bind reversibly with 1-NPN with dissociation constants in the micromolar range. Figure 4 shows the binding curves, and their relative linearisation, using Scatchard plots. In most cases the points fit a straight line, but for OBP47 and OBP19 the plot is curved upwards, allowing the evaluation of two binding constants. This phenomenon cannot be attributed to the presence of two binding sites on the same protein unit, as structural studies have clearly shown a compact structure for insect OBPs enclosing a single binding pocket. However, most of these OBPs will be present as dimers in the conditions used for the binding experiments [14], and it has been shown that when OBPs crystallize as dimers, the two monomeric structures, and therefore their binding pockets, cannot be considered equivalent [38]. Whether the phenomenon of two binding constants is observed in ligand-binding experiments will be dependent on (1) the degree of asymmetry of the dimer and (2) the dissociation constant for the equilibrium monomer/dimer. In this respect it is worth recalling that the concentration of OBPs in the insect's sensillum lymph is extremely high (in the millimolar range), making any equilibrium strongly shifted towards the formation of dimers.

In a second series of experiments we measured the affinity of each OBP for a number of potential ligands in competitive binding assays, using 1-NPN as the fluorescent reporter.

We used both volatiles present in the environment, including some reported, or supposed, to be active on mosquitoes, as well as homologous series of synthetic ligands, such as benzoates, in order to define the structural requirements of an ideal ligand for each protein. The natural compounds we tested included (*E*)-2-hexenal, citronellal, geranyl acetate and indole, which have all been reported to specifically activate olfactory receptors of *A. gambiae* [10]. In particular, indole has been reported as a ligand for OBP1, on the basis that silencing the gene encoding OBP1 suppresses electrophysiological response to indole, but not to other odorants [19]. Other compounds, such as 1-octen-3-ol, decanal, 6-methyl-5-hepten-2-one, menthol, linalool and *p*-cresol, were found to be constituents of human sweat and to produce electrophysiological and behavioural responses in mosquitoes [2, 3]. DEET,

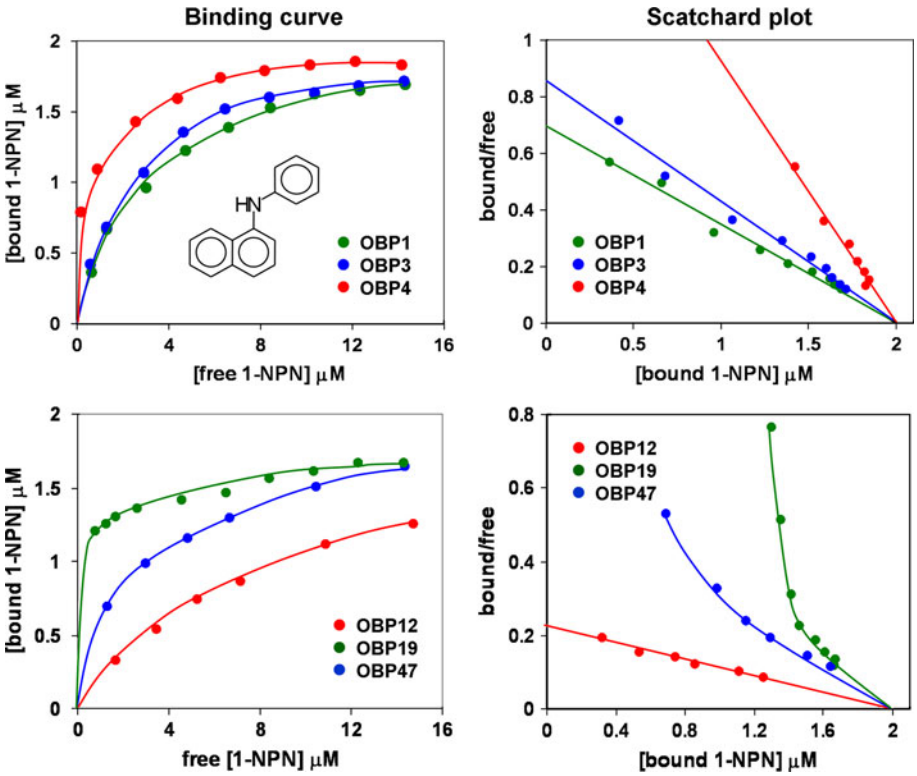

Fig. 4 Binding curves of 1-NPN and relative Scatchard plot analyses. A 2 µM solution of the protein in Tris-buffer was titrated with 1 mM solution of 1-NPN in methanol to final concentrations of 2–16 µM. Dissociation constants (average of three replicates) were OBP1: 4.7 µM (SD 2.5); OBP3, 2.3 µM (SD 1.6); OBP4, 1.6 µM (SD 1.2); OBP12, 8.9 µM (SD 0.3); OBP19, 2.1 µM (SD 0.6); OBP47, 2.7 µM (SD 0.2)

Table 1 Binding of pure organic compounds to selected recombinant OBPs of *A. gambiae*

Ligand	OBP1			OBP3			OBP4			OBP12			OBP19			OBP47		
	IC_{50}	Int	K_i	IC_{50}	Int	K_i	IC_{50}	Int	K_i	IC_{50}	Int	K_i	IC_{50}	Int	K_i	IC_{50}	Int	K_i
Alcohols																		
(*Z*)-3-Hexenol		82			67			72										
1-Octanol		91			66			91									91	
1-Octen-3-ol		82			71			71									71	
1-Nonanol		88			62			65										
1-Decanol		73			63			58										
Linalool		78			66			73									73	
Menthol	21	57	**20.2**	17	51	**13.9**	6	31	**4.6**							6	31	**5.0**
1-Dodecanol		77			64		14	46	**10.7**							14	46	**11.8**
3,7-Dimethyloctanol								61										
a-Pentylcinnamyl alcohol											77			70				
Farnesol							12	52	**9.2**		112		2.2	26	**1.8**			
Retinol							4	26	**3.1**		55		5.2	30	**4.2**			
Aldehydes and ketones																		
Hexanal		83			61			97									85	
(*E*)-2-Hexenal		84			64			73										
Octanal		102			66		8	42	**6.1**					73			73	
(*E*)-2-Octenal		68		12	43	**9.8**		68										
Nonanal	17	51	**16.3**	16	50	**13.1**	10	44	**7.6**		130			54			71	
(*E*)-2-Nonenal	13	46	**12.5**	12	41	**9.8**	20	55	**15.3**								72	
Decanal		80			86		17	51	**13.0**							17	51	**14.3**
(−)-citronellal	5.5	40	**5.3**	14	45	**11.5**	18	53	**13.7**				16	51	**12.9**	18	53	**15.1**
Benzaldehyde		96			60			65						93			69	
α-Pentyl cinnamaldehyde							3.5	16	**2.7**	7.4	27	**7.3**						
6-Methyl-5-hepten-2-one		88			63			78									87	
Jasmone		80			64			78										
Geranylacetone					67			72									93	
Retinal								73			110			72				
Carboxylic acids																		
Pentanoic acid														71				
Heptanoic acid														80				
Octanoic acid								60										
7-Octenoic acid		92			68			77									77	
Nonanoic acid														80				
Undecanoic acid														67				
Benzoates																		
Ethyl benzoate								59			121		17	52	**13.7**			
Butyl benzoate								62			82		1.3	17	**1.0**			
Hexyl benzoate							3.5	19	**2.7**		61		6.5	31	**5.2**			
Octyl benzoate							20	54	**15.3**		92		16	50	**12.9**			
3,7-Dimethyloctyl benzoate							3	30	**2.3**	20	53	**19.8**	1.7	29	**1.4**			
3-Hexyl benzoate										11.7	39	**11.6**	20	52	**16.1**			
4-Methylpentyl benzoate							1.8	12	**1.4**	12	43	**11.9**	6	25	**4.8**			
p-Isopropylphenyl benzoate							10	39	**7.6**	15.5	49	**15.3**	5.8	36	**4.7**			
Butyl *p*-tert-butylbenzoate										15	48	**14.9**	1.4	19	**1.1**			
Phenyl benzoate											104		16	51	**12.9**			
p-Tolyl benzoate											82			55				

Table 1 continued

Ligand	OBP1			OBP3			OBP4			OBP12			OBP19			OBP47		
	IC_{50}	Int	K_i	IC_{50}	Int	K_i	IC_{50}	Int	K_i	IC_{50}	Int	K_i	IC_{50}	Int	K_i	IC_{50}	Int	K_i
2-Phenylethyl benzoate													9.5	42	**7.7**			
Benzyl benzoate											87							
p-tert-Butylphenyl benzoate							6	29	**4.6**	10	41	**9.9**	5	30	**4.0**			
Butyl *p*-nitrobenzoate								56					11	46	**8.9**			
Isobutyl *p*-nitrobenzoate											84			64				
Aromatic compounds																		
m-Cresol														62				
p-Cresol		71						71									71	
p-tert-Butylbenzophenone							4	17	**3.1**	6	21	**5.9**	7.5	21	**6.0**	3.2	17	**2.7**
Phenylbenzylhydrazine										4.7	28	**4.7**						
Indole		87			70		20	58	**15.3**		86			60		20	58	**16.8**
Methyl cinnamate														67				
Butyl cinnamate											60			57				
o-Hydroxybenzaldehyde														58				
p-tert-butyl benzaldehyde											88			57				
N-p-isopropylphenyl-*p*-hydroxybenzimine							8	34	**6.1**									
4-Hydroxy-4'-isopropylazobenzene							2.5	6	**1.9**	1.1	1	**1.1**	5.2	28	**4.2**	1.4	5	**1.2**
2-Pyrrolyl-*p*-methyl-azobenzene										2	2.5	**2.0**	3.5	15	**2.8**	5	16	**4.2**
N,N-diethyl-*m*-toluamide (DEET)		85			69			85									85	
Others																		
(*E*)-*β*-Farnesene								73										
3,7-Dimethyloctyl acetate											108		12	45	**9.7**			
Icaridin														65				

Solutions of protein and fluorescent probe 1-NPN, both at the concentration of 2 μM, were titrated with 1 mM solution of each ligand in methanol to final concentrations of 2–16 μM. For each protein, we report the fluorescence intensity (*Int*) measured at the maximal ligand concentration (16 μM) as percent of the initial fluorescence, the concentration of ligand halving the initial fluorescence intensity (IC_{50}), where applicable, and the relative dissociation constant (K_i) calculated as described in "Materials and methods"

Icaridin and thymol were also tested as representatives of mosquito repellents. Table 1 shows the IC_{50} values (the concentration of the ligand halving the initial fluorescence value) and the calculated inhibition constant (K_i) where possible for the OBP/ligand combinations. For weaker ligands, where IC50 values could not be measured, we report fluorescence intensity measured at the highest concentration of ligand (16 μM) as percent of the initial value. Figure 5 shows the displacement curves obtained with a selected set of ligands for each OBP.

As expected, on the basis of similar studies performed with other OBPs, a broad specificity can be observed for the OBPs of *A. gambiae*, with each protein preferentially binding to several related compounds. OBP1, OBP3 and OBP4 and, to some extent, OBP47 show some similarities in their binding spectra, being focussed on terpenoids of medium size and some structurally related molecules. Figure 5 shows the affinities of these four OBPs to the same set of ligands. Thus, the best ligand for OBP1 is citronellal, OBP3 binds 2-octenal and 2-nonenal, and several compounds bind rather strongly to OBP4, with menthol being the best among the natural volatiles. Menthol is also the best natural ligand of OBP47, despite the marked structural differences between these two OBPs. We can also observe that the structures of citronellal and menthol have the same number of carbon atoms, arranged in the same terpene topology, the main difference being an additional bond, which closes the open chain of citronellal into the ring of menthol. 2-Octenal, on the other hand, differs from citronellal by two side methyl groups, apart from the position of the double bond.

Figure 6 shows an alignment of the amino acids of OBPs 1, 3 and 4, together with the three-dimensional structure of OBP1 [39] and a model of OBP4. The sequences of OBP1 and OBP3 are very similar to each other, as are their *Drosophila* orthologues OS-E and OS-F, these in turn differ markedly from the mosquito OBP4 and its *Drosophila* orthologue LUSH. The binding cavity of OBP1 is lined with several branched amino acid residues, most of them conserved in OBP3 (also predicted to fold in

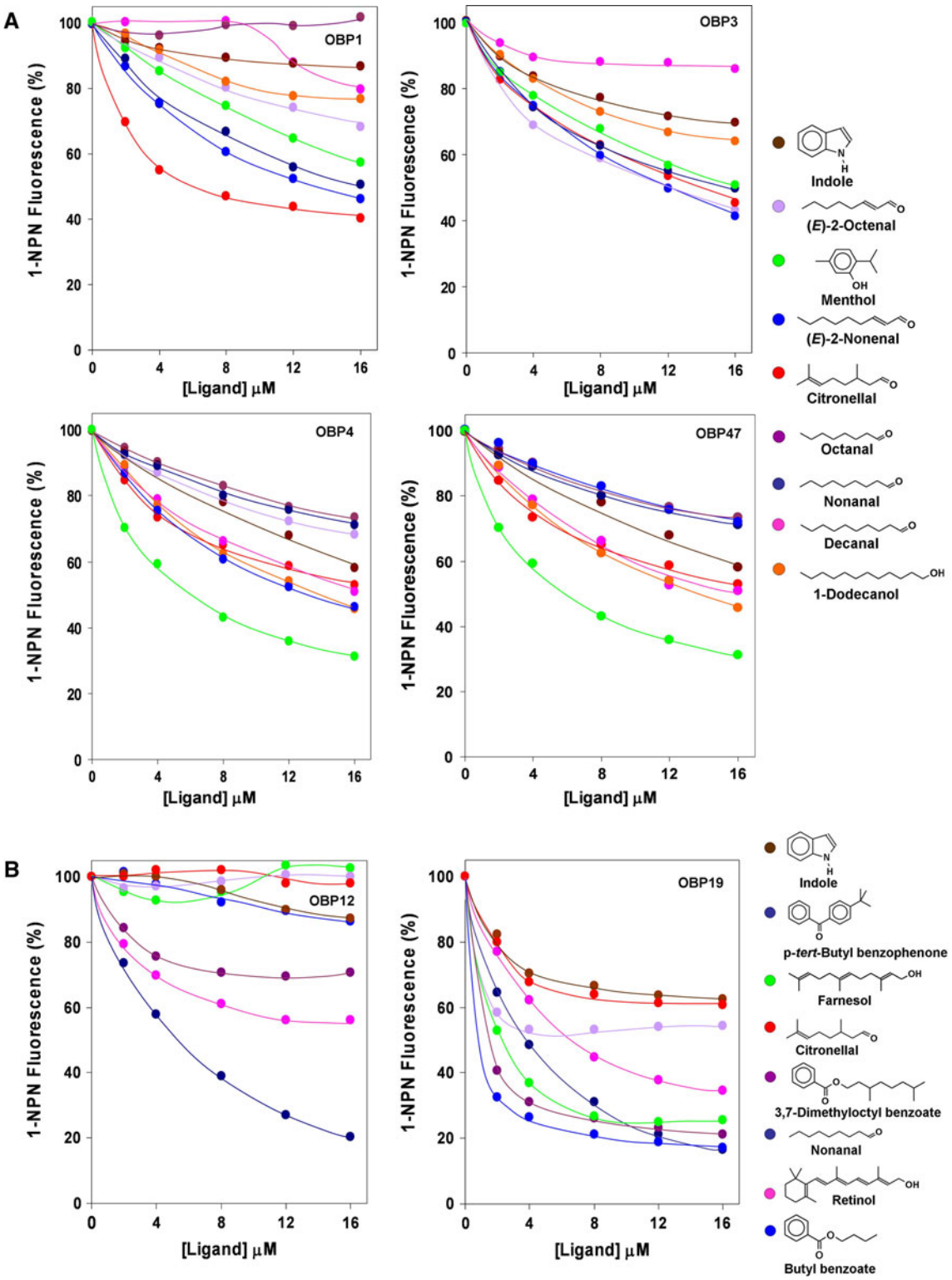

Fig. 5 Binding of selected ligands to recombinant OBPs of *A. gambiae*. A mixture of the protein and 1-NPN in Tris-buffer, both at a concentration of 2 μM, was titrated with 1 mM solutions of each competing ligand to final concentrations of 2–16 μM. Fluorescence intensities are reported as percent of the values in the absence of competitor. The calculated dissociation constants and the binding data relative to all the ligands tested are reported in Table 1

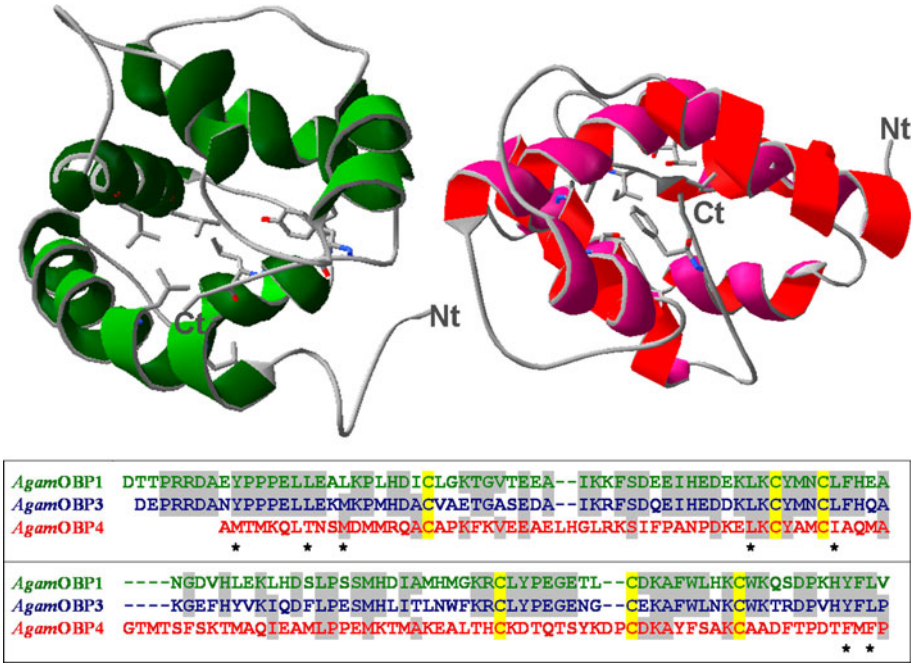

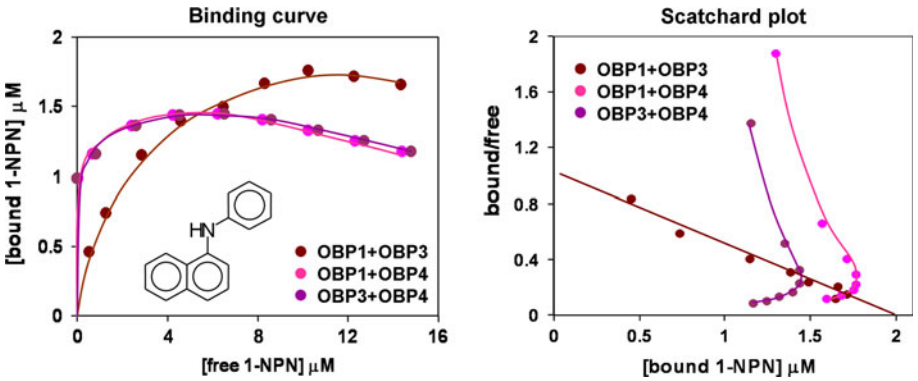

Fig. 6 Three-dimensional structure of OBP1 [39] and a model structure of OBP4. The model of OBP3 is very similar to the structure of OBP1, while the folding of OBP4 appears significantly different, particularly with reference to the residues lining the binding sites. The alignment of the three proteins shows high similarity between OBP1 and OBP3. Asterisks indicate amino acids present in the binding pockets. The sequence and folding differences between OBP1 and OBP4 provide structural support to the different spectra of binding observed with the two proteins

Fig. 7 Binding curves of 1-NPN and relative and Scatchard plot analyses measured with binary mixtures of OBPs 1, 3 and 4. A solution of two proteins in Tris-buffer, both at the concentration of 2 µM, was titrated with 1 mM solution of 1-NPN in methanol to final concentrations of 2–16 µM. The mixture of OBP1 and OBP3 shows a regular behaviour with a binding curve in agreement with that predicted and a linear Scatchard plot. Mixtures containing OBP4 have binding curves with a maximum around 4 µM of free probe and Scatchard plots that cannot be analysed. Such behaviour indicates cooperative interactions between OBP1 and OBP4 and between OBP3 and OBP4, as predicted in previous reports [22]

a similar way) and which can interact with the terpene skeleton of ligands, such as citronellal and menthol. The two tyrosine residues, conserved in OBP1 and OBP3 and present near the amino and carboxy termini, and at the entrance of the binding cavity, might establish hydrogen bonds with the terpenoids and related compounds. Two other OBPs 12 and 19 seem to be tuned to larger molecules. In particular, OBP12 seems to prefer aromatic compounds and OBP19 binds terpenoids of larger size with farnesol being its best natural ligand.

When analysing the results of our binding experiments, we were surprised that none of the OBPs showed significant affinity to indole. Only with OBP4 and OBP47 were we able to calculate dissociation constants of around 16 µM, whilst with the other proteins indole could not displace the fluorescent probe more than 30% even at the highest concentration used. This is not consistent with the previously reported observation that silencing the gene for OBP1 suppresses response to indole in *A. gambiae* [19]. One possible explanation was that the OBPs can associate in heterodimers, with binding properties different from those of their components. Some such association between OBPs has been observed in *A. gambiae*. In particular, co-immunoprecipitation has indicated that there are interactions between OBP1 and OBP4 [22], although there is no evidence that the two proteins are expressed in the same

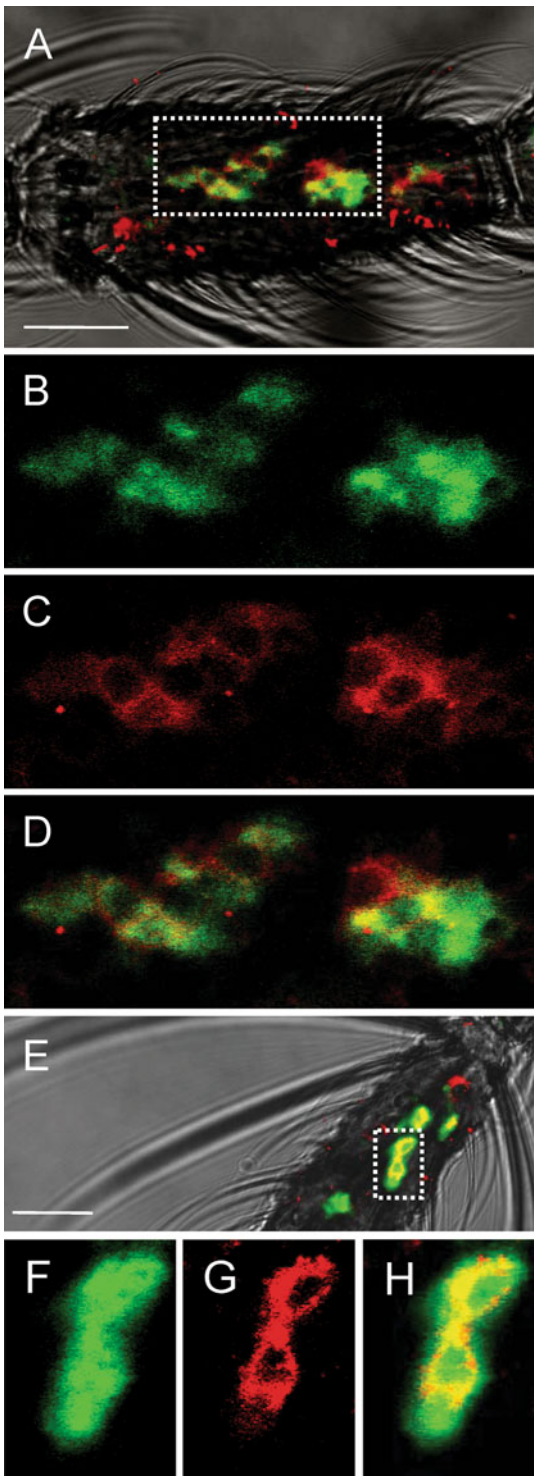

Fig. 8 Co-expression of OBP1 and OBP4 in the antenna of female *A. gambiae*. Two-colour WM-FISH was performed on antennae using DIG-labelled OBP1 and biotin-labelled OBP4 antisense RNAs. Hybridisation signals were visualised using detection systems indicating OBP1-positive cells by *red* fluorescense (**c**, **g**) and OBP4-labelled cells by *green* fluorescence (**b**, **f**). In most cases the OBP1- and the OBP4-probes label the same cells (**a**, **d**, **e**, **h**), indicating a co-expression of the two proteins. OBP1- and OBP4-expressing cells are shown on segment 8 (**a**–**d**) and segment 13 (**e**–**h**) of two different female antennae. All pictures represent single optical planes taken by a confocal laser scanning microscope. In **a** and **e** the *red* and *green* fluorescence channels have been overlaid with the transmitted light channel. The *boxed* areas in **a** and **e**, respectively, are shown at higher magnifications below the corresponding image with the *green* (**b**, **f**) and the *red* (**c**, **g**) fluorescence channels presented separately or as an overlay (**d**, **h**). *Scale bars*: 20 μm

sensilla. Co-localisation of OBPs has been reported in *D. melanogaster*, where OS-E, OS-F and LUSH are found in the same sensilla [34, 35], and since these three OBPs are the orthologues of *A. gambiae* OBP1, OBP3 and OBP4, respectively [40, 41] we decided to measure the affinity of 1-NPN to binary mixtures of the three proteins.

The results for the binding of 1-NPN to binary mixtures of two OBPs are shown in Fig. 7. A mixture of equimolar amounts of OBP1 and OBP3 gave a binding curve not different from the sum of the those obtained with the individual proteins and a rather linear Scatchard plot indicating that there is no cooperativity effect. However, when one of the partner proteins was OBP4, the binding curve exhibited an unexpected behaviour, rising very sharply at the beginning, reaching a maximum at low concentrations of ligand and then decreasing significantly at higher concentrations. The relative Scatchard analyses are also unusual and do not allow any calculation of affinity constants. The decrease in bound 1-NPN, whilst its total concentration is increasing can only be explained if there is interaction between the two OBPs. From the experiments performed with individual proteins, we measured values for binding of OBP4 to 1-NPN that are nearly double those of OBP1 or OBP3 (similar between the two). Thus, the Scatchard plots seen in Fig. 7 can be best explained by assuming that 1-NPN binds first to OBP4 (with the stronger affinity), then, as the concentration of the free probe increases, the ligand is transferred from OBP4 to the other partner protein. The total amount of bound ligand, therefore, does not change, or could even increase, but the observed fluorescence decreases. This mechanism requires an active interaction between the two OBPs.

We have measured displacement of 1-NPN by indole, using a mixture of OBP1 and OBP4, but could not detect large decrement of the fluorescence. This result does not necessarely indicate that indole does not bind to the proteins, as the fluorescent probe displaced from one OBP could partly bind to the other, thus compensating the displacement effect. This effect would be particularly evident for molecules of 1-NPN bound to OBP1 (low fluorescence yield) that would be tranfered to OBP4 (high fluorescence yield). If indole is detected not by OBP1 alone, but rather by the heterodimer OBP1/OBP4, this would mean that, like OS-E and LUSH of *Drosophila*, the *A. gambiae* OBPs 1 and 4 would have to be present in the same sensilla. To test for co-localisation of OBP1 and OBP4 in the same

sensillum, we used two-colour WM-FISH. Female antennae were simultaneously probed with specific DIG-labelled OBP1- and biotin-labelled OBP4-antisense RNA probes. Then using detection systems leading to red (DIG) and green (biotin) fluorescence allowed visualisation of cells, with both transcripts for the two OBPs by means of confocal laser scanning microscopy (Fig. 8a, b). Both red-labelled cells expressing OBP1 (Fig. 8c, g), and green-labelled cells positive for OBP4 (Fig. 8b, f) were detected and in the overlay of the red and green fluorescence in distinct optical planes (Fig. 8d, h); most of the OBP1-positive cells were also positive for OBP4, strongly indicating co-expression of both OBPs in these cells. This result makes it likely that OBP1 and OBP4 are secreted simultaneously from supporting cells into the sensillum lymph and supports the notion that OBP1/OBP4 dimers are of functional relevance.

Our results, together with previous reports, strongly indicate that OBPs can form heterodimers in the sensillum lymph, with binding characteristics different from those of the individual proteins. This phenomenon, which could be widespread in insects, will effectively increase the number of binding proteins for odours and pheromones, expanding their chemical communication potential.

Acknowledgments We thank Drs. Dan Woods (Inscent, Inc., Irvine, CA) and Marika Walter (University of California, Irvine, CA) for access to their *A. gambiae* antennal cDNA library, which was used as starting material for the isolation of the ORFs of the OBPs analysed in this report. We also thank Maria Calzetta for technical assistance in rearing and manipulation of mosquito samples. This study was supported by a European Union grant (FP7/2007-2013,Grant Agreement No. FP7-222927) to FRD, JK, KI, LF and PP.

References

1. Justice RW, Dimitratos S, Walter MF, Woods DF, Biessmann H (2003) Sexual dimorphic expression of putative antennal carrier protein genes in the malaria vector *Anopheles gambiae*. Insect Mol Biol 12:581–594
2. Logan JG, Birkett MA (2007) Semiochemicals for biting fly control: their identification and exploitation. Pest Manag Sci 63:647–657
3. Logan JG, Birkett MA, Clark SJ, Powers S, Seal NJ, Wadhams LJ, Mordue Luntz AJ, Pickett JA (2008) Identification of human-derived volatile chemicals that interfere with attraction of *Aedes aegypti* mosquitoes. J Chem Ecol 34:308–322
4. Corbel V, Stankiewicz M, Pennetier C, Fournier D, Stojan J, Girard E, Dimitrov M, Molgó J, Hougard JM, Lapied B (2009) Evidence for inhibition of cholinesterases in insect and mammalian nervous systems by the insect repellent deet. BMC Biol 7:47
5. Cheng SS, Liu JY, Tsai KH, Chen WJ, Chang ST (2004) Chemical composition and mosquito larvicidal activity of essential oils from leaves of different *Cinnamomum osmophloeum* provenances. J Agric Food Chem 14:4395–4400
6. Chang KS, Tak JH, Kim SI, Lee WJ, Ahn YJ (2006) Repellency of *Cinnamomum cassia* bark compounds and cream containing cassia oil to *Aedes aegypti* (Diptera: Culicidae) under laboratory and indoor conditions. Pest Manag Sci 62:1032–1038
7. Gu HJ, Cheng SS, Huang CG, Chen WJ, Chang ST (2009) Mosquito larvicidal activities of extractives from black heartwood-type *Cryptomeria japonica*. Parasitol Res 105:1455–1458
8. Zhang A, Klun JA, Wang S, Carroll JF, Debboun M (2009) Isolongifolenone: a novel sesquiterpene repellent of ticks and mosquitoes. J Med Entomol 46:100–106
9. Biessmann H, Nguyen QK, Le D, Walter MF (2005) Microarray-based survey of a subset of putative olfactory genes in the mosquito *Anopheles gambiae*. Insect Mol Biol 14:575–589
10. Allison F, Carey AF, Wang G, Su C-Y, Zwiebel LJ, Carlson JR (2010) Odorant reception in the malaria mosquito *Anopheles gambiae*. Nature 464:66–72
11. Wang G, Carey AF, Carlson JR, Zwiebel LJ (2010) Molecular basis of odor coding in the malaria vector mosquito *Anopheles gambiae*. Proc Natl Acad Sci USA 107:4418–4423
12. Vogt RG, Riddiford LM (1981) Pheromone binding and inactivation by moth antennae. Nature 293:161–163
13. Vogt RG (2003) Biochemical diversity of odor detection: OBPs, ODEs and SNMPs. In: Blomquist GJ, Vogt RG (eds) Insect pheromone biochemistry and molecular biology. Elsevier, London, pp 391–446
14. Pelosi P, Zhou JJ, Ban LP, Calvello M (2006) Soluble proteins in insect chemical communication. Cell Mol Life Sci 63:1658–1676
15. Grosse-Wilde E, Svatos A, Krieger J (2006) A pheromone-binding protein mediates the bombykol-induced activation of a pheromone receptor in vitro. Chem Senses 31:547–555
16. Xu P, Atkinson R, Jones DN, Smith DP (2005) *Drosophila* OBP LUSH is required for activity of pheromone-sensitive neurons. Neuron 45:193–200
17. Laughlin JD, Soo TH, Jones DNM, Smith DP (2008) Activation of pheromone-sensitive neurons is mediated by conformational activation of pheromone binding protein. Cell 133:1255–1265
18. Matsuo T, Sugaya S, Yasukawa J, Aigaki T, Fuyama Y (2007) Odorant-binding proteins OBP57d and OBP57e affect taste perception and host-plant preference in *Drosophila sechellia*. PLoS Biol 5:e118
19. Biessmann H, Andronopoulou E, Biessmann MR, Douris V, Dimitratos SD, Eliopoulos E, Guerin PM, Iatrou K, Justice RW, Kröber T, Marinotti O, Tsitoura P, Woods DF, Walter MF (2010) The *Anopheles gambiae* odorant binding protein 1 (AgamOBP1) mediates indole recognition in the antennae of female mosquitoes. PLoS ONE 5(3):e9471
20. Pelletier J, Guidolin A, Syed Z, Cornel AJ, Leal WS (2010) Knockdown of a mosquito odorant-binding protein involved in the sensitive detection of oviposition attractants. J Chem Ecol 36:245–248
21. Biessmann H, Walter MF, Dimitratos S, Woods DF (2002) Isolation of cDNA clones encoding putative odorant binding proteins from the antennae of the malaria-transmitting mosquito, *Anopheles gambiae*. Insect Mol Biol 11:123–132
22. Andronopoulou E, Labropoulou V, Douris V, Woods DF, Biessmann H, Iatrou K (2006) Specific interactions among odorant-binding proteins of the African malaria vector *Anopheles gambiae*. Insect Mol Biol 15:797–811
23. Iatrou K, Biessmann H (2008) Sex-biased expression of odorant receptors in antennae and palps of the African malaria vector *Anopheles gambiae*. Insect Biochem Mol Biol 38:268–274
24. Xu PX, Zwiebel LJ, Smith DP (2003) Identification of a distinct family of genes encoding atypical odorant-binding proteins in the malaria vector mosquito, *Anopheles gambiae*. Insect Mol Biol 12:549–560

25. della Torre A, Fanello C, Akogbeto M, Dossou-yovo J, Favia G, Petrarca V, Coluzzi M (2001) Molecular evidence of incipient speciation within *Anopheles gambiae* s.s. in West Africa. Insect Mol Biol 10:9–18
26. Coluzzi M, Sabatini A, della Torre A, Di Deco MA, Petrarca V (2002) A polytene chromosome analysis of the *Anopheles gambiae* species complex. Science 298:1415–1418
27. Ban LP, Scaloni A, Brandazza A, Angeli S, Zhang L, Yan Y, Pelosi P (2003) Chemosensory proteins of *Locusta migratoria*. Insect Mol Biol 12:125–134
28. Calvello M, Guerra N, Brandazza A, D'Ambrosio C, Scaloni A, Dani FR, Turillazzi S, Pelosi P (2003) Soluble proteins of chemical communication in the social wasp *Polistes dominulus*. Cell Mol Life Sci 60:1933–1943
29. Kyhse-Andersen J (1984) Electroblotting of multiple gels: a simple apparatus without buffer tank for rapid transfer of proteins from polyacrylamide to nitrocellulose. J Biochem Biophys Methods 10:203–209
30. Dani FR, Francese S, Mastrobuoni G, Felicioli A, Caputo B, Simard F, Pieraccini G, Moneti G, Coluzzi M, Della Torre A, Turillazzi S (2008) Exploring proteins in *Anopheles gambiae* male and female antennae through MALDI mass spectrometry profiling. PLoS One 3:e2822
31. Arnold K, Bordoli L, Kopp J, Schwede T (2006) The SWISS-MODEL Workspace: a web-based environment for protein structure homology modelling. Bioinformatics 22:195–201
32. Guex N, Peitsch MC (1997) SWISS-MODEL and the Swiss-PdbViewer: an environment for comparative protein modelling. Electrophoresis 18:2714–2723
33. Schwede T, Kopp J, Guex N, Peitsch MC (2003) SWISS-MODEL: an automated protein homology-modeling server. Nucleic Acids Res 31:3381–3385
34. Hekmat-Scafe DS, Steinbrecht RA, Carlson JR (1997) Coexpression of two odorant-binding protein homologs in *Drosophila*: implications for olfactory coding. J Neurosci 17:1616–1624
35. Shanbhag SR, Hekmat-Scafe D, Kim MS, Park SK, Carlson JR, Pikielny C, Smith DP, Steinbrecht RA (2001) Expression mosaic of odorant-binding proteins in *Drosophila* olfactory organs. Microsc Res Tech 55:297–306
36. Prestwich GD (1993) Bacterial expression and photoaffinity labeling of a pheromone binding protein. Protein Sci 2:420–428
37. Kruse SW, Zhao R, Smith DP, Jones DN (2003) Structure of a specific alcohol-binding site defined by the odorant binding protein LUSH from *Drosophila melanogaster*. Nat Struct Biol 10:694–700
38. Tegoni M, Campanacci V, Cambillau C (2004) Structural aspects of sexual attraction and chemical communication in insects. Trends Biochem Sci 29:257–264
39. Wogulis M, Morgan T, Ishida Y, Leal WS, Wilson DK (2006) The crystal structure of an odorant binding protein from *Anopheles gambiae*: evidence for a common ligand release mechanism. Biochem Biophys Res Commun 339:157–164
40. Vogt RG (2002) Odorant binding protein homologues of the malaria mosquito *Anopheles gambiae*; possible orthologues of the OS-E and OS-F OBPs of *Drosophila melanogaster*. J Chem Ecol 28:2371–2376
41. Zhou JJ, He XL, Pickett JA, Field LM (2008) Identification of odorant-binding proteins of the yellow fever mosquito *Aedes aegypti*: genome annotation and comparative analyses. Insect Mol Biol 17:147–163